Biosensors and Bioelectronics 41 (2013) 150–156

Contents lists available at SciVerse ScienceDirect

Biosensors and Bioelectronics

journal homepage: www.elsevier.com/locate/bios

Fluorometric enzymatic autoindicating biosensor for H_2O_2 determination based on modified catalase

Estefania Ortega, Susana de Marcos, Javier Galbán*

Bioanalytical sensors group (GBA), Analytical Chemistry Department, Faculty of Sciences, Aragon Institute of Nanosciences of Aragon (INA), University of Zaragoza, Pedro Cerbuna 12, Zaragoza 50009, Spain

ARTICLE INFO

Article history:
Received 24 March 2012
Received in revised form
20 July 2012
Accepted 1 August 2012
Available online 23 August 2012

Keywords:
Autoindicating biosensor
Fluorescence
Catalase
Hydrogen peroxide
Ruthenium compound
O_2 quenching

ABSTRACT

Our general aim is to develop reversible optical biosensors which can be used for continuous monitoring. In this paper we propose a biosensor for H_2O_2 determination. The bioreceptor is catalase (Cat) previously linked to a Ruthenium O_2-sensitive fluorophore (Cat–Ru). It is based on the reversible H_2O_2 disproportionation into O_2 and H_2O.

First, the fluorescent-enzymatic system was optimized for batch measurements (linear response ranges from 1×10^{-4} to, at least, 1×10^{-3} M H_2O_2). Because of its reversibility, the same enzyme aliquot can be used for performing the whole calibration step (and the subsequent determination). Secondly, the optical sensor was prepared by Cat–Ru immobilization in a polyacrylamide film. The sensor permits H_2O_2 determination in a similar concentration range as in batch mode and can be used during at least 1 month. A mathematical model has also been developed which permits the effect of the experimental parameters to predict. The model also explains the sensor behavior if different fluorophores are used, and shows that the analytical signal only slightly depends on the initial concentration of the O_2 in the sample.

Finally an alternative sensor is presented based on a commercially available O_2 fluorescence sensor linked to catalase. This system gives an analytical behavior similar to that shown for the Cat–Ru sensor.

1. Introduction

In spite of the substantial amount of work done in optical sensor research, it is difficult to find a biochemical receptor/optical transducer scheme which can be used for a device permitting the continuous monitoring of a chemical compound in clinical or environmental samples. Perhaps one of the most interesting alternatives is based on using biochemical receptors that, in the appropriate concentration range, give easily reversible reactions and have autoindicating optical properties (intrinsic or acquired).

Some kinds of transport proteins (binding globulins, calmodulin, lectins or periplasmic binding proteins) are between the most important groups of receptors which are being studied for continuous monitoring biosensors. These proteins lack of proper autoindicating capabilities so different methodological alternatives have been proposed for improving them. This is: the use of competitive schemes involving a fluorophore (Ballerstadt and Schultz, 1997; Ballerstadt et al., 2004); the linkage of an environmentally sensitive fluorophore (De Lorimier et al., 2002; Yoon et al., 2011); or the joining of two fluorophores for producing energy transfer (Medintz et al., 2004; Crochet et al., 2010)

Enzymes, mainly those having flavin or heme groups as cofactors, have also abilities for being used in continuous monitoring biosensors. Their capabilities can be summarized as follows:

1. Autoindicating properties. Flavoenzymes have intrinsic fluorescence (and absorption) in the visible region due to the presence of the flavin group (Massey, 2000); their autoindicating abilities are partially or fully quenched by the surrounding aminoacid structure but they can be recovered after the linkage of specific fluorophores, as fluorescein or coumarin (Odaci, et al., 2009; Galban et al., 2012). Heme-proteins have molecular absorption properties due to their hemegroup. During the enzymatic reaction, the central iron ion oxidation state becomes altered and, as a consequence, its molecular absorption spectrum changes (Nienhaus and Nienhaus, 2005). This change in absorbance can be used for autoindicating purposes.
2. Concentration range. Enzymes usually give similar or higher linear response ranges than transport proteins and they can be easily tuned by choosing an appropriate enzyme concentration. Their detections limits are usually conditioned by their spectroscopic properties (Sanz et al., 2007a).

* Corresponding author. Tel.: +34 976761291; fax: +34 976761292.
E-mail address: jgalban@unizar.es (J. Galbán).

0956-5663/$ - see front matter © 2012 Elsevier B.V. All rights reserved.
http://dx.doi.org/10.1016/j.bios.2012.08.001

3. Reversibility: Flavoenzymes and metalloproteins are intrinsically reversible, but they need a regenerating substance. Flavoenzymes are regenerated by O_2; since this compound is present in the majority of the samples, these enzymes are, in fact, reversible. The case of metalloproteins is different. Most of them need an additional reducer for regeneration (as is the case of peroxidase (Sanz et al., 2007b) or hemoglobin), but Catalase (Cat) represents an interesting exception.

The active center of Cat is composed of a hemegroup containing a ferric (Fe(III)) central ion; in addition, Cat contains a NADPH group. This enzyme catalyzes substrate oxidation by organic peroxides. Catalase is also able to disproportionate hydrogen peroxide into water and oxygen:

$$2H_2O_2 \xrightarrow{\text{Catalase}} 2H_2O + O_2 \quad (1)$$

Kinetically, this reaction is complex (Ogura and Yamazaki, 1983; Lardinois et al., 1996) but, considering the aim of this paper, it comprises two steps. First, the Fe(III) is oxidized by H_2O_2 to give the so-called Compound-I (CpI), a porphyrin π-cation radical containing Fe^{IV}:

$$Cat + H_2O_2 \xrightarrow{k_1} CpI\left(Fe^{IV=0}\right) + H_2O \quad (2)$$

In the second step another H_2O_2 molecule reduces the CpI to the initial oxidation state.

$$CpI\left(Fe^{IV=0}\right) + H_2O_2 \xrightarrow{k_2} Cat + H_2O + O_2 \quad (3)$$

The overall process is so quick that it is not possible to observe changes in the molecular absorption spectra due to the Cat–CpI–Cat transition. As can be seen, Cat self-regenerates during the reaction and, in consequence, it can be used as a bioreceptor for a H_2O_2 continuous monitoring system.

H_2O_2 is a very interesting analyte in several kinds of biochemical and environmental samples. In biochemistry, in addition to its well known importance in aging, this compound plays a role as an intracellular messenger (Veal et al., 2007), in the response of the immune system (Niethammer et al., 2009) and there is evidence that it contributes to neurodegeneration in diseased states (O'Brien et al., 2007). In the environmental field, the compound is used (sometimes in combination with organic peroxides) as a water disinfectant as an alternative to chlorine or to chlorine dioxide. Colorimetric or fluorometric methods for H_2O_2 determination are usually based on two mains schemes: (A) H_2O_2 enzymatic oxidation with peroxidase (or peroxidase mimics (Gao et al., 2011)) in the presence of an adequate reagent (for example, the ABTS method Cadarso et al., 2008), and (B) the Fe(II) oxidation to Fe(III) and a later Fe(III) complexing with Xylenol Orange (FOX method) or other reagents (Bou et al., 2008). These methods give good sensitivity but they are irreversible, so it is difficult to use in continuous monitoring systems. To the best of our knowledge, reaction (1) has only been used for designing electrochemical biosensors (O'Brien et al., 2007; Sezginturk et al., 2005; Campanella et al., 1998; Campanella et al., 2003). In this paper we propose a different indicating scheme based on detecting the O_2 formed with an O_2-sensitive fluorophore which has been previously linked to the catalase.

2. Material and methods

2.1. Apparatus

Steady state fluorescence measurements and contour plot (3D) spectral measurements were carried out with a Photon Technology International (PTI) Time Master spectrometer (TM-2/2003). For lifetime measurements this instrument has a N_2 laser (GL-3300) that pumps a dye laser (plugged in to a frequency doubler for working with lower wavelengths) as a radiation source and a stroboscopic system as the detector. 3D spectral measurements were carried out with a Perkin-Elmer LS 50B luminometer. 3.5 mL Hellma quartz cuvettes with 10 mm path length were used.

The chemically modified enzyme was separated from the modifier excess using a low-pressure chromatography system. This consists of a glass column (13 × 1 cm) filled with Sephadex G-50. A peristaltic pump (M312 MiniPlus3) supplied the eluent.

An optical Foxy-R Oxygen Sensor (Ocean Optics), which is based on the O_2 collisional quenching of fluorescence, was used for monitoring dissolved oxygen during the enzymatic reaction. Optical fibers carried both the excitation light produced by the blue LED (450 nm) and the fluorescence generated to the detector.

The flow system was a modified version of a system previously designed in our laboratory (see Supplementary Material section, Fig. S1).

The Cat–O_2 sensor consists on a center holed (0.3 × 0.4 mm) 0.36 × 20 mm polytetrafluoroethylene tube closed by two septum caps. The PAA-catalase polymer is located at the bottom and the Foxy-R Oxygen Sensor is inserted through the top cover.

2.2. Reagents

pH 8.5 and 9 0.1 M carbonate solutions were prepared from solid $NaHCO_3$ and Na_2CO_3. 13500 IU · mg^{-1} lyophilized solid *Bovine liver* Catalase (Cat) EC 232-577-1 (Sigma-Aldrich, C40) was used throughout the experimental study. The ruthenium salt solution (Ru salt) was prepared by dissolving 1.42 mg of Tris(2,2′-bipyridine)dichlororuthenium(II) hexahydrate (Fluka 93307) in 100 μL of dimethylsulfoxide (DMSO). The ruthenium chemical modifier solution (CM–Ru) was prepared by dissolving 2 mg of Bis(2,2′-bipyridine)-4′-methyl-4-carboxybipyridine-Ru N-succinimidyl ester-bis (hexafluoro-phosphate) (Sigma 96631) in 1 mL of dimethylsulfoxide (DMSO). Hydrogen peroxide stock solution (33% w/v) was supplied by Panreac. Hydrogen peroxide stock solution (16.75 M obtained by Permanganate titration) was supplied by Scharlab.

APEG-Membranes® (polyethylene glycol–cellulose amine modified membrane) and Immobilon-P® (polyvinylidene difluoride membrane) were supplied by RAPP Polymere and Millipore, respectively. Polyacrylamide membranes (PAA) were synthesized from acrylamide, bis-acrylamide and ammonium persulfate (Sigma-Aldrich A3553, M7279 and A3678, respectively) and N,N,N,N-tetramethylenediamine (TEMED, from BioRad).

2.3. Linking procedure

Mixture 1 (Mix-1): About 10 mg of Cat were dissolved in 400 μL pH 8.5 carbonate solution and mixed with 100 μL CM–Ru. The mixture was allowed to react in darkness at room temperature during 90 min. The excess of CM–Ru was separated from the chemically modified Cat (Cat–Ru) using a chromatographic system. pH 9 carbonate solution was used as eluent (flow rate: 1.5 mL min^{-1}). The Cat–Ru was recovered in a volumetric flask and made up to 5 mL with pH 9 carbonate solution.

Mixture 2 (Mix-2): About 12 mg of Cat were dissolved in 250 μL pH 8.5 carbonate solution and mixed with 200 μL CM-Ru solution. The mixture was allowed to react in darkness at room temperature during 120 min.

2.4. Catalase–Ru immobilization in PAA (sensor film preparation)

75 mg acrylamide and 5 mg bis-acrylamide were dissolved in 200 μL Mix-2. Then 4 μL ammonium persulfate solution (10%) was added. After bubbling with N_2 during a few minutes to

remove dissolved oxygen, 0.4 μL TEMED were added before the mixture was spread into a glass cast ($1.2 \times 1.2 \times 1$ mm). After being covered with a glass slide, the mixture was left to react during 30 min. The sensor film was kept in pH 9 carbonate solution.

2.5. Catalase–Ru immobilization in APEG and Inmobylon-P (sensor film preparation)

A piece of APEG-membrane was cut to the appropriate dimensions. 10 μL Mix-2 were spotted on the membrane and dried. This last step was repeated twice for each side of the membrane. The sensor film was kept in pH 9 carbonate solution.

Immobilon-P membrane must be previously activated. A piece was wet in 100% methanol for 20 s and then washed with milliQ water for 2 min before being equilibrated in pH 9 carbonate solution (for 5 min). 10 μL Mix-2 were then spotted on the membrane and dried. This last step was repeated twice for each side. The sensor film was kept in pH 9 carbonate solution.

2.6. Measurement procedure

Lifetime measurements. The cuvette was filled with Cat–Ru solution Mix-1 ([Cat–Ru]$=8.0 \times 10^{-6}$ M). The decay curves were then obtained and fitted to an exponential function (the best fit was determined when $0.9 < \chi^2 < 1.2$). To obtain the Ru lifetime in the absence of O_2, the same procedure was used after bubbling with N_2 for removing O_2.

Measurements in batch. 400 μL Mix-1 and 1600 μL pH 9 carbonate solution were added to the quartz cuvette ([Cat–Ru]$=1.32 \times 10^{-6}$ M). The mixture was submitted to continuous stirring and the fluorescent intensity was monitored at 617 nm ($\lambda_{exc}=467$ nm). Then 30 μL of the analyte solution was added to the cuvette. A fast intensity decrease from an initial (F_0) to a minimum value (F_{min}) followed by a gradual increase was observed. Two analytical parameters were used: $\Delta F_{min}=F_0-F_{min}/F_{min}$ and the absolute value of the signal area ($A_{\Delta F}$).

For the "One Cat–Ru aliquot working" methodology, 500 μL of Cat–Ru solution and 1.5 mL pH 9 carbonate solution were added to the quartz cuvette ([Cat–Ru]$=1.41 \times 10^{-6}$ M). Volumes of analyte solution were then added to the cuvette (10–60 μL), the fluorescence also being monitored at 600 nm ($\lambda_{exc}=467$ nm). Similar conditions were used when the Ru salt was measured.

Cat–Ru Sensor films. The pH 9 carbonate solution was flowed across the flow cell at 0.5 mL min^{-1} and the fluorescence intensity was monitored at 600 nm ($\lambda_{exc}=450$ nm). When signal stabilization was reached, 2.5 mL of the analyte solution were injected in FIA mode.

Cat–O_2 sensor. 500 μL of the solution to be tested are located in a 1 mL Eppendorf tube (Fig. 1). Then the Cat–O_2 probe is immersed and the F_{min} is obtained. The F_0 is measured from a blank solution.

3. H_2O_2 determination using Cat–Ru in solution

3.1. Fluorescence properties of Cat–Ru

The spectrum of catalase after being linked to the Ru–chelate (Cat–Ru) shows the intrinsic spectroscopic properties due to aminoacids, the intrinsic fluorescence maximum at 400 nm (excitation at 310 nm), due to NADPH, and the additional fluorescence maximum at 617 nm (excitation at 467 nm) due to the Ru compound (see Supplementary Material Fig. S2).

Table 1 shows the fluorescence lifetime of both CM–Ru and Cat–Ru in the presence (τ_0) and in the absence (τ'_0) of O_2. These

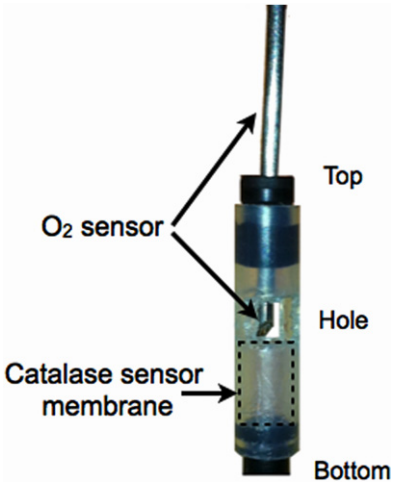

Fig. 1. Cat–O_2 sensor system.

Table 1
Lifetime obtained for Cat–Ru, CM–Ru and sensor film in the O_2 presence (τ_0, $[O_2]_0=2.2 \times 10^{-4}$ M) and absence (τ'_0, $[O_2]$ concentration lower than 10^{-5} M). From τ_0 and τ'_0 the Sterm–Volmer constants (K_{SV}) have been obtained (results are the average of 5 determinations).

	τ_0 (ns)	τ'_0 (ns)	K_{SV} (M^{-1})	k_q (M^{-1} s^{-1})
Cat–Ru	402 ± 5	462 ± 9	678 ± 15	$1.47(\pm 0.04) \cdot 10^9$
CM–Ru	418 ± 7	502 ± 12	913 ± 27	$1.82(\pm 0.07) \cdot 10^9$
Sensor film	122 ± 4	209 ± 9	*	*

* Non evaluated

were obtained using the lifetimes measurement system previously described. They show that the O_2 quenching is even produced when the Ru–chelate is linked to catalase.

The Sterm–Volmer equation for collisional quenching is given by

$$\frac{F'_0}{F_0}=\frac{\tau'_0}{\tau_0}=1+K_{SV}[O_2]_0=1+\gamma_q k_q \tau'_0[O_2]_0 \approx 1+k_q\tau'_0[O_2]_0 \quad (4)$$

γ_q being the quenching efficiency (which is very close to 1 when O_2 is the quencher (Eftink, 1991)), k_q being the rate constant for quenching and K_{sv} being the Sterm–Volmer constant. From Eq. (4) and the data in Table 1, the K_{sv} and k_q for CM–Ru and Cat–Ru have been obtained. These results indicate that

$$\frac{k_q^{\text{Cat–Ru}}}{k_q^{\text{CM–Ru}}}=0.81$$

Both k_q values are comparable, which is an indication that the fluorescence quenching by O_2 is responsible for the Cat–Ru signal. The small difference between these values (about 20%) can be explained by the findings of Johnson and Yguerabide (1985). They studied the k_q values for free and protein bound fluorophores and found that the k_q can be reduced by up to a half when the fluorophore is bound to a protein (the bigger the protein the stronger the k_q reduction). They also indicated that higher reductions suggest that the fluorophore is hidden from O_2 and, consequently, the fluorophore is in the inner part of the protein. According to this, in Cat–Ru the fluorophore is in the outer part of the catalase.

3.2. Mathematical model describing the analytical method.

Fig. 2 shows schematically the fluorescence changes produced when hydrogen peroxide is added to a solution containing Cat–Ru.

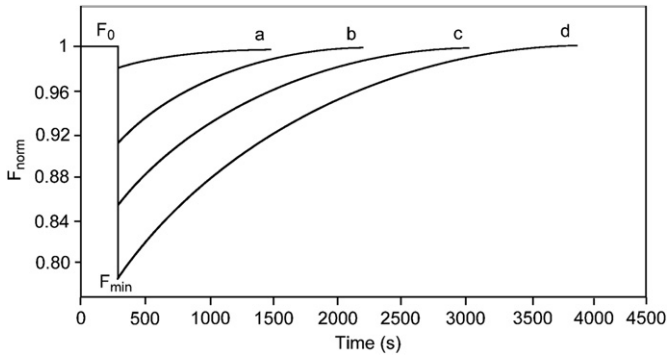

Fig. 2. Cat–Ru fluorescence intensity versus time along the enzymatic reaction using different H_2O_2 concentrations: (a) Blank; (b) 3.0×10^{-4} M; (c) 7.0×10^{-4} M; (d) 1.0×10^{-3} M (pH 9; [Cat–Ru] $\approx 1.0\times10^{-6}$ M). Fluorescence intensity has been normalized (F_{norm}) with the initial value (F_0).

After the analyte addition, a sudden fall in fluorescence intensity is observed (up to a minimum value, F_{min}); from the minimum, the fluorescence increases again until the initial fluorescence signal is recovered. According to the Cat/H_2O_2 reaction mechanism, the initial fluorescence fall is due to O_2 formation (which quenches the Cat–Ru fluorescence) and the subsequent increase is due to O_2 diffusion from the surrounding atmosphere to the solution until the initial O_2 concentration is reached (k_{dif} being the diffusion constant). This fact was confirmed by monitoring the variation of O_2 with the oxygen sensor (see Fig. S3 in the Supplementary Material section).

Considering the kinetic mechanism, a mathematical model relating the fluorescence intensity change with the H_2O_2 concentration can be developed. Before the reaction, the Cat–Ru fluorescence is quenched by the dissolved oxygen present in the solution.

$$\frac{F_0'}{F_0} = 1 + K_{SV}^{Cat-Ru}[O_2]_0 \tag{5}$$

When H_2O_2 is added the O_2 increases by the enzymatic reaction (1) and decreases by diffusion, so the fluorescence intensity at each moment (F) is given by:

$$\frac{F_0'}{F} = 1 + K_{SV}^{Cat-Ru}([O_2]_0 + [O_2]_e) \tag{6}$$

$[O_2]_e$ being the excess in the O_2 concentration (regarding $[O_2]_0$) present at each moment in the solution. Combining (5) and (6) gives

$$\Delta F = \frac{F_0 - F}{F} = \frac{K_{SV}^{Cat-Ru}}{1 + K_{SV}^{Cat-Ru}[O_2]_0}[O_2]_e = Q_{SV}[O_2]_e \tag{7}$$

the Q_{SV} term represents the part of the overall system sensitivity depending on the fluorophore used. Now the $[O_2]_e$ has to be related with the analyte concentration $[H_2O_2]_0$. According to the enzyme reaction/diffusion kinetic

$$\frac{d[O_2]_e}{dt} = k_2[CpI][H_2O_2] - k_{O_2}^{s,g}[O_2]_e \tag{8}$$

$k_{O_2}^{s,m}$ being the solution to gas O_2 diffusion coefficient. Details on this differential equation solution are given in supplementary material section, the result being

$$[O_2]_e = [H_2O_2]_0\left(\frac{\left(\frac{k_1k_2}{k_1+k_2}\right)[Cat]_0}{2\left(\frac{k_1k_2}{k_1+k_2}\right)[Cat]_0 - k_{O_2}^{s,g}}\right)\left(e^{-k_{O_2}^{s,g}t} - e^{-2\left(\frac{k_1k_2}{k_1+k_2}\right)[Cat]_0 t}\right) \tag{9}$$

This equation indicates that the $[O_2]_e$ and, in consequence ΔF, linearly depends on the $[H_2O_2]_0$ concentration at any time during the enzymatic reaction. Throughout, we will use two analytical parameters which are linearly related to the $[H_2O_2]_0$ (both are deduced in the Supplementary Material section).

1) The ΔF values of the minimum (ΔF_{min}) given by

$$\Delta F_{min} = \frac{1}{2}[H_2O_2]_0 Q_{SV}\left(\frac{P_{s,g}}{1-P_{s,g}}\right)\ln\left(\frac{1}{P_{s,g}}\right)$$

$$P_{s,g} = \frac{2\left(\frac{k_1k_2}{k_1+k_2}\right)}{k_{O_2}^{s,g}}[Cat]_0 \tag{10}$$

$P_{s,g}$ being a term representing the enzyme kinetic to mass transfer quotient rate.

2) The absolute value of the area of the ΔF versus time representation ($A_{\Delta F}$)

$$A_{\Delta F} = [H_2O_2]_0\frac{Q_{SV}}{2K_{O_2}^{s,g}} \tag{11}$$

As could be expected, the $A_{\Delta F}$ does not depend on the catalase concentration as the ΔF_{min} does. Both equations give the analytical keys for designing methods and optical sensors based on this methodology.

3.3. Analytical optimization and figures of merit

Only two variables need to be optimized: pH and catalase concentration. Table S1 in supplementary material shows how the $A_{\Delta F}$ and the ΔF_{min} are nearly independent on the pH for values ranging from 6 to 9 (which are the typical for enzymatic measurement).

Catalase concentration is included in the $P_{s,g}$ value. When the effect of the logarithmic term is considered negligible compared to the $(P_{s,g}/(1-P_{s,g}))$, then two limiting situations can be established

1) For low catalase concentration

$$2\left(\frac{k_1k_2}{k_1+k_2}\right)[Cat]_0 << k_{O_2}^{s,g} \Rightarrow \Delta F_{min} = \frac{1}{2}[H_2O_2]_0 Q_{SV} P_{s,g}\ln\left(\frac{1}{P_{s,g}}\right) \tag{12}$$

indicating that ΔF_{min} linearly depends on the catalase concentration.

2) For High enzyme concentration

$$2\left(\frac{k_1k_2}{k_1+k_2}\right)[Cat]_0 >> k_{O_2}^{s,g} \Rightarrow \Delta F_{min} = \frac{1}{2}[H_2O_2]_0 Q_{SV}\ln(P_{s,g}) \tag{13}$$

then ΔF_{min} becomes nearly independent of the catalase concentration and the sensitivity reaches its highest value. Fig. 3 shows the experimental results obtained which match with these predictions. This figure shows that the $A_{\Delta F}$ does not depend on the catalase concentration; however, kinetically speaking the higher the catalase concentration the shorter the reaction time. When ΔF_{min} is used as the analytical parameter, in order to achieve the highest sensitivity, catalase concentrations above 1.6×10^{-6} M should be used.

Eq. (4) shows that K_{SV} linearly depends on the k_q, γ and τ'_0. As is well known, the k_q value was initially deduced by Smoluchowski. While this equation was later improved by Collins y Kimbal (Eftink, 1991), for the majority of the situations the Smoluchowski equation (simplified to steady-state measurements) can be used.

$$k_q = 4\pi R_0 D\frac{N_a}{1000}\left[1 + \frac{R_0}{\sqrt{\pi Dt}}\right] \approx 4\pi R_0 D\frac{N_a}{1000} \tag{14}$$

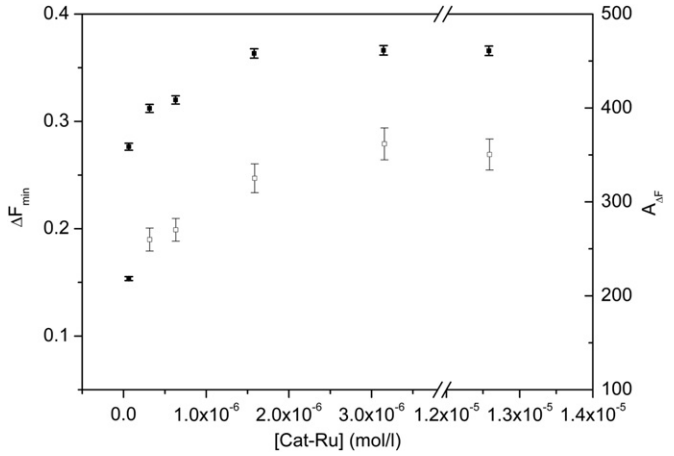

Fig. 3. Cat–Ru concentration effect on the analytical parameters: ■ ΔF_{min}; □ $A_{\Delta F}$ (pH 9; $[H_2O_2]=1.3\times10^{-3}$ M).

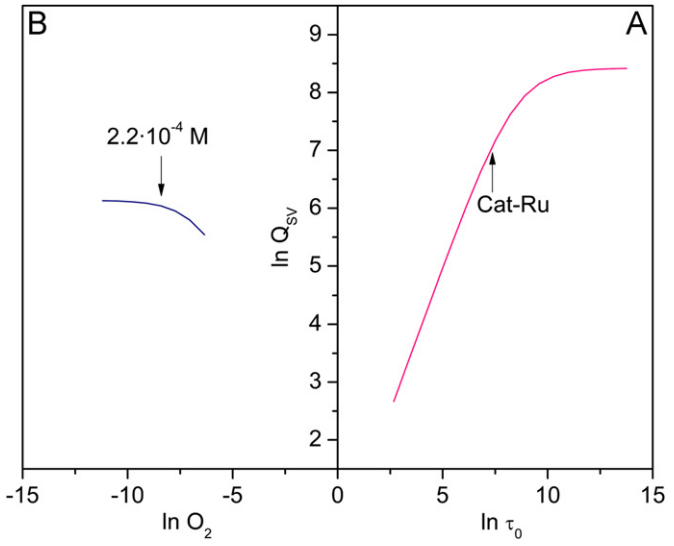

Fig. 4. (A) Simulated effect of $[O_2]_0$ on the Q_{SV} value ($K_{SV}=678\ M^{-1}$); (B) Simulated effect of τ'_0 on the Q_{SV} value ($k_q=1.5\times10^9\ M^{-1}s^{-1}$; $[O_2]_0=2.22\times10^{-4}$ M) using a double logarithmic representation.

R_0 being the distance between the fluorophore and the O_2 (usually, the sum of both radii), D being the sum of the diffusion coefficients of both compounds and N_a being the Avogadro number. As can be seen, for fluorophores having similar radii (i.e., similar molecular weight) the k_d value can be considered constant. Then, for similar fluorophores the most important parameter to be considered should be τ'_0. Fig. 4A shows an estimation of the τ'_0 effect on the Q_{SV} value (considering $k_q=1.47\times10^9\ M^{-1}s^{-1}$ and $[O_2]_0=2.2\times10^{-4}$ M); for the sake of clarity a double-logarithmic representation has been used. As can be seen, if fluorophores having a longer lifetime than Ru were used, the Q_{SV} would increase and, in consequence, the method sensitivity also; however this increase is limited. In fact, for very high τ'_0 values, Q_{SV} becomes independent of K_{SV}

$$Q_{SV}=\frac{K_{SV}}{1+K_{SV}[O_2]_0}\approx\frac{K_{SV}}{K_{SV}[O_2]_0}=\frac{1}{[O_2]_0} \quad (15)$$

Fig. 4A indicates that using a fluorophore having a longer fluorescence lifetime than the Ru compound used, the Q_{SV} can be increased by about one order of magnitude. We have considered this possibility in our method design. As far as we know, the only commercially available fluorophores having longer lifetimes than the Ru compound (or metalloprophyrins) are Eu (III) chelates (metalloporphyrins having similar lifetime to the Ru). However, the fluorescence of these compounds (Hemmilä and Laitala, 2005) is almost unaffected by O_2 ($\gamma_q\sim0$) so the Ru seems to be the most appropriate. Metalloporphyrins have also long lifetimes but they are similar to that of the Ru compounds.

Eq. (10) also indicates that the method sensitivity changes linearly with Q_{SV} and this, for its part, depends on the $[O_2]_0$ present in the medium and the K_{SV}. According to Eq. (7), the higher the $[O_2]_0$, the lower the Q_{SV} and, in consequence, the lower the method sensitivity. However, considering the K_{SV} value given in Table 1, the effect of the $[O_2]_0$ is in reality slight. This is clearly depicted in Fig. 4B which represents the theoretical Q_{SV} variation with $[O_2]_0$ (the $[O_2]_0$ in water at 25 °C is 2.2×10^{-4} M; $K_{SV}=678\ M^{-1}$). As can be seen, if the $[O_2]_0$ is reduced by half or is increased twofold, the slope of the calibration line changes less than 5%. It is necessary to change the $[O_2]_0$ by one order of magnitude if a noticeable change in Q_{SV} is to be observed. This result also shows the robustness of the method to $[O_2]_0$ changes.

In the optimal conditions, a calibration study was performed using ΔF_{min} and $A_{\Delta F}$. Both parameters change linearly with the H_2O_2 concentration in the range from 1.0×10^{-4} M to, at least, 1.2×10^{-3} M. The calibration lines obtained by the least-square method are as follows (see Figs. S4 and S6 in the Supplementary Material section; calibration lines obtained using other conditions are shown in Figs. S5 and S7, and in Table S3)

$$\Delta F_{min}=119[H_2O_2,M]-0{,}002 \quad r=0.998 \quad (16)$$

$$A_{\Delta F}=99279[H_2O_2,M]+1.4 \quad r=0.998 \quad (17)$$

The RSDs ($n=5$) obtained for the 1.31×10^{-3} M were 1.2% and 4.7% for ΔF_{min} and $A_{\Delta F}$, respectively. The limits of detection (calculated according to the IUPAC criteria) were $2{,}5\times10^{-5}$ M and $3{,}0\times10^{-5}$ M for ΔF_{min} and $A_{\Delta F}$ respectively.

As has been indicated above, the Catalase/H_2O_2 kinetic is complex. In fact, for high H_2O_2 concentrations the analyte can produce reversible inhibition (and even, irreversible inactivation) by the formation of a new enzyme compound (Compound III) (Lardinois et al., 1996). In our opinion, this behavior explains the lost of linearity at the highest $[H_2O_2]$ of the calibration study.

3.4. One Cat–Ru aliquot working

One of the most interesting aspects of this method is that the analytical system is fully reversible. This means that after H_2O_2 consumption and O_2 diminution to its initial value, the same catalase solution can be used again for the measurement of a new H_2O_2 aliquot. In theory, this process could be repeated as many times as is needed, and the calibration line could be obtained with just one catalase aliquot. The only consideration to be taken into account is that after a new analyte aliquot is added, the enzyme becomes diluted; however, while the catalase concentration remains in the plateau shown in Fig. 3 (i.e., while Eq. (13) can be applied), this dilution will not affect the method. In order to demonstrate this capability a calibration study was performed using a single aliquot of Cat–Ru. The calibration lines obtained (see figures in the Supplementary Material section) by least-square method being

$$\Delta F_{min}=248\ [H_2O_2,M]+0.01 \quad r=0.990 \quad (18)$$

$$A_{\Delta F}=241145[H_2O_2,M]-2.2 \quad r=0.995 \quad (19)$$

As can be seen, the slope of both parameters are consistent with those obtained by the sequential calibration studies (Eqs. (16) and (17)). The supplementary material section also shows that this

method can be applied when the Ru compound has not been previously linked to the catalase.

4. Sensor film for Cat–Ru biosensor

4.1. Mathematical model describing the biosensor

Cat–Ru was immobilized in a PAA membrane and then placed in a flow cell. Working in FIA mode, the analytical signal obtained is similar to that obtained in batch mode, the only difference being that the fluorescence minimum appears later and is more dependent on the analyte mass transport step (Fig. 5).

Eq. (8) describes the $[O_2]_e$ variation along time for the H_2O_2 determination in solution. When the Ru–Cat is immobilized into a membrane, a different mathematical model has been developed modeling the analytical parameters. For this case, the $A_{\Delta F}$ gave greater experimental precision than ΔF_{min} so this parameter is proposed for quantification. The obtained equation was (see Supplementary material section).

$$A_{\Delta F} \approx \frac{1}{2} Q_{SV} \left(\frac{P_{s,m}}{1+P_{s,m}} \right) \frac{V_m}{Q} [H_2O_2]_0 \quad (20)$$

$P_{s,m}$ being similar to $P_{s,g}$ but replacing the diffusion coefficient $k_{O_2}^{s,g}$ by $k_{O_2}^{s,m}$, the latter being the membrane to solution O_2 diffusion coefficient, and Q and V_m being the carrier sample flow and, sample volume respectively. This indicates that the area is proportional to the analyte concentration.

4.2. Parameter optimization

Most of the biosensors we have previously designed and built have been based on enzyme entrapment in polyacrylamide gels (PAA). In this paper we have also tested two commercial supports previously described (see Section 2). The most important advantage of these supports compared to PAA is that the Cat–Ru becomes immobilized on the solid surface so the mass transport rate increases. On the other hand, these supports have two drawbacks: (1) the amount of enzyme which can be immobilized is less than in PAA, and (2) the enzyme chemical groups involved in the immobilization are the same as those of the enzyme used for Ru linkage. With APEG we could not get any signal; using Immobilon-P both the fluorescence intensity and its variation was very low (see Fig. S14 in Supplementary Material).

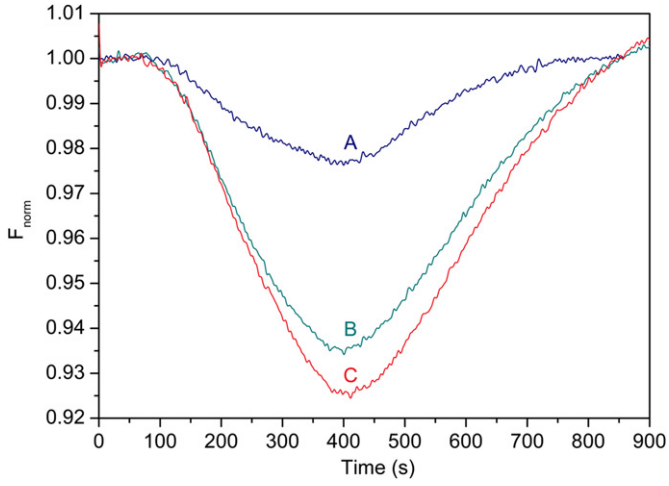

Fig. 5. Variation of the fluorescence intensity of the sensor film during the enzymatic reaction using different H_2O_2 concentrations: (A) 1.7×10^{-3} M; (B) 1.3×10^{-2} M; (C) 1.7×10^{-2} M (pH 9; [Cat–Ru]$=9.9 \times 10^{-5}$ M).

Although the flow cell dimensions do not explicitly appear in the mathematical model, in order to deduce Eq. (20) it is necessary to ensure that the flow cells volume will be as low as possible in order to minimize the signal size (i.e. obtaining a higher $F_{0,min}$). Initially the flow cell we used had a free volume (available for sample) of about 220 μL ($0.5 \times 1 \times 0.45$ cm). Using this volume a very low $F_{0,min}$ value was observed. Lower volumes were obtained using similar cells in which the total height had been reduced using silicone. The better ΔF_{min} value was obtained using 100 μL volume ($0.5 \times 1 \times 0.2$ cm), this being the smallest volume we could accurately use.

Eq. (20) predicts how the sample volume and the flow rate affect on the analytical signal. The experimental results confirm the model (see Fig. S15 in Supplementary Material). According to this, the sample volume should be large; in contrast, the flow rate should be kept as low as possible.

4.3. Analytical figures of merit

As shown in the previous section the optimal pH is 9. Therefore, the same conditions were used as in solution. The catalase concentration affects the analytical response and the stability of the sensor film. For high concentrations of catalase the reaction was faster but the stability of the sensor film decreased. A concentration of 1.00×10^{-4}–7.00×10^{-4} M was chosen. Using these optimized conditions, the calibration line is linear from 5×10^{-4} M up to (at least) $1{,}4 \times 10^{-2}$ M (see Supplementary Material, Fig. S16).

Finally, a study has been carried out in order to evaluate the sensor lifetime. In the experimental conditions indicated in Section 2.6, periodic measurements of a 1×10^{-4} M H_2O_2 were performed during one month (every 2 day). The relative standard deviation of these measurements were 3,5% ($n=15$).

5. The Cat–O_2 sensor: an alternative H_2O_2 optical sensor

Fiber-optic oxygen sensors based in fluorescence are commercially available. These sensors consisting in long-lifetime fluorophores (in some cases, Ru chelates similar to that used in this paper) immobilized in crystalline materials (i.e., sol–gel). In order to transform this O_2 sensor in a H_2O_2 sensor, catalase should be coupled to that system.

Taking this in mind, we have built a H_2O_2 sensor using a PPA support containing immobilized free-catalase (Cat–O_2 sensor). Several devices were initially tested and finally that shown in Fig. 1 was chosen. The mechanism of the fluorescence change is similar to that of the Cat–Ru sensor, so the model can also be applied. Catalase concentration was again studied. Obviously the higher the concentration the faster the reaction, however there is a limit imposed by the physical characteristics of the PAA polymer. Finally a 1×10^{-6} M can be recommended as the optimum. We also observed that the PAA-probe relative position highly affects the method sensitivity; both should be as near as possible avoiding a direct contact between them.

This device has been designed to be used as an immersion probe. Fig. S17 in the supplementary material section shows the shape of the $F=f(t)$ representations obtained. As can be seen a sudden intensity change is observed followed by stabilization. Since the final stabilization time and the final signal depend on the sample container size, we decided to use the ΔF_{min} as the measurement parameter. Fig. S18 in the supplementary material section shows the calibration line obtained by the successive immersion of the Cat–O_2 probe in solutions containing different H_2O_2 concentration. As can be seen the method sensitivity and the linear response range are similar to that obtained with the

Cat–Ru sensor, so this system can be use as an alternative to the Cat–Ru sensor.

6. Conclusions

In this paper we have presented an autoindicating biosensor based on catalase which is able to determine hydrogen peroxide. This sensor is fully reversible, does not need any chemical for regeneration, is less prone to interferences (mainly, from organic peroxides) than other methods for H_2O_2 determination and can work autonomously for at least one month. Since catalase is easily coupled to many oxidase-type enzymatic reactions involving classical clinical substrates such as glucose, cholesterol, lactic acid and many others, this work opens the door to a new optical sensor family based on proteins. These sensors could be candidates for continuous monitoring of these parameters in biological fluids.

Acknowledgments

Authors thanks the Spanish Ministerio de Economía y Competitividad (MINECO) (project CTQ2012-34774), Gobierno de Aragon-Obra Social "La Caixa" (project GA-LC-036/2011) and DGA-Fondo Social Europeo (DGA-FSE) for the financial support.

Appendix A. Supporting information

Supplementary data associated with this article can be found in the online version at http://dx.doi.org/10.1016/j.bios.2012.08.001.

References

Ballerstadt, R., Schultz, J., 1997. Analytica Chimica Acta 345, 203–212.
Ballerstadt, R., Polak, A., Beuhler, A., Frye, J., 2004. Biosensors and Bioelectronics 19, 905–914.
Bou, R., Codony, R., Tres, A., Deckler, E.A., Guardiola, F., 2008. Analytical Biochemistry 377, 1–15.
Campanella, L., Favero, G., Sammartino, M.P., Tomassetti, M., 1998. Talanta 46, 595–606.
Campanella, L., Favero, G., Giancola, D., Tomassetti, M., 2003. Journal of Pharmaceutical and Biomedical Analysis 32, 737–751.
Cadarso, V.J., Fernández-Sánchez, C., Llobera, A., Darder, M., Dominguez, C., 2008. Analytical Chemistry 80, 3498–3501.
Crochet, A.P., Kabir, M.M., Francis, M.B., Paavola, C.D., 2010. Biosensors and Bioelectronics 26, 55–61.
De Lorimier, R., Smith, J., Dwyer, M., Looger, L.L., Soli, K.M., Paavola, C.D., Rizk, S.S., Sadigov, S., Conrad, D.W., Loew, L., Hellinga, H.W., 2002. Protein Science 11, 2655–2675.
Eftink, M.R., 1991. In: Lakowicz, J.R. (Ed.), Topics in Fluorescence Spectroscopy, Vol. 2. Plenum Press, New York, pp. 53–126.
Galban, J., Sanz, I., Ortega, E., del Barrio, M., de Marcos, S., 2012. Analytical and BioanalyticalChemistry 402, 3039–3054.
Gao, Y., Wang, G.N., Huang, H., Hu, J.J., Shah, S.M., Su, X.G., 2011. Talanta 85, 1075–1080.
Hemmilä, I., Laitala, V., 2005. Journal of Fluorescence 15, 529–542.
Johnson, D.A., Yguerabide, J., 1985. Biophysical Journal 48, 949–955.
Lardinois, O.M., Mestdagh, M.M., Rouxhet, P.G., 1996. Biochimica et Biophysica Acta 1295, 222–238.
Massey, V., 2000. Biochemical Society Transactions 28, 283–296.
Medintz, I.L., Anderson, G.P., Lassman, M.E., Goldman, E.R., Bettencourt, L.A., Mauro, J.M., 2004. Analytical Chemistry 76, 5620–5629.
Nienhaus, K., Nienhaus, G.U., 2005. In: Nienhaus, G.R. (Ed.), Protein-Ligands Interactions: Methods and Applications (Methods in Molecular Biology), 305. Humana Press, New Jersey, pp. 215–242.
Niethammer, P., Grabher, C., Look, A.T., Mitchison, T.J., 2009. Nature 459, 996–999.
O'Brien, K.B., Killoran, S.J., O'Neill, R.D., Lowry, J.P., 2007. Biosensors and Bioelectronics 22, 2994–3000.
Odaci, D., Gacal, B.N., Gacal, B., Timur, S., Yagci, Y., 2009. Biomacromolecules 10, 2928–2934.
Ogura, Y., Yamazaki, I., 1983. Journal of Biochemistry 94, 403–408.
Sanz, V., de Marcos, S., Galban, J., 2007a. Biosensors and Bioelectronics 22, 956–964.
Sanz, V., de Marcos, S., Galban, J., 2007b. Biosensors Bioelectronics 22, 2876–2883.
Sezginturk, M.K., Goktuk, T., Dinckaya, E., 2005. Biosensors and Bioelectronics 21, 684–688.
Veal, E.A., Day, A.M., Morgan, B.A., 2007. Molecular Cell 26, 1–14.
Yoon, H., Ahn, J.-H., Barone, P.W., Yum, K., Sherma, R., Boghossian, A.A., Han, J.-H., Strano, M.S., 2011. Angewandte Chemie International Edition 50, 1828–1831.